Environmental Science Nano

Delivering metribuzin from biodegradable nanocarriers: Assessing herbicidal effects for soybean plant protection and weed control

Journal:	*Environmental Science: Nano*
Manuscript ID	EN-ART-08-2024-000784.R2
Article Type:	Paper

Delivering metribuzin from biodegradable nanocarriers: Assessing herbicidal effects for soybean plant protection and weed control

Vanessa Takeshita[1]; Felipe F. Oliveira[2]; Alvaro Garcia[3]; Nubia Zuverza-Mena[4]; Carlos Tamez[4]; Brian C. Cardoso[1]; Camila W. Pinácio[1]; Blaire Steven[5]; Jacquelyn LaReau[5]; Carlos E. Astete[3]; Cristina M. Sabliov[3]; Leonardo F. Fraceto[6]; Valdemar L. Tornisielo[1]; Christian O. Dimkpa[4]; Jason C. White[4]

[1]Center of Nuclear Energy in Agriculture, University of São Paulo, Piracicaba, SP 13416-000, Brazil; [2]Department of Plant Pathology & Nematology, Superior School of Agriculture "Luiz de Queiroz", University of São Paulo, Piracicaba, SP 13418-900, Brazil; [3]Biological & Agricultural Engineering, Louisiana State University and LSU Ag Center, Baton Rouge, LA 70808, United States; [4]Department of Analytical Chemistry, The Connecticut Agricultural Experiment Station, New Haven, CT 06511, United States; [5]Department Environmental Science and Forestry, The Connecticut Agricultural Experiment Station, New Haven, CT 06504, United States; [6]Institute of Science and Technology, São Paulo State University (UNESP), Sorocaba, SP 18087-180, Brazil.

Environmental Significance Statement

Although polymeric nanoparticles are very efficient in delivering herbicides and controlling weeds, few reports on crop concerns can be found in the literature. This study explores the aspects related to the efficient delivery of the herbicide metribuzin by polymeric nanoformulations, with efficient weed control, while observing the least damage caused to crops and soil organisms. Dose reduction is the achievement of these polymeric nanoformulations and the key to sustainable herbicide applications.

Delivering metribuzin from biodegradable nanocarriers: Assessing herbicidal effects for soybean plant protection and weed control

Vanessa Takeshita[1*]; Felipe F. Oliveira[2]; Alvaro Garcia[3]; Nubia Zuverza-Mena[4]; Carlos Tamez[4]; Brian C. Cardoso[1]; Camila W. Pinácio[1]; Blaire Steven[5]; Jacquelyn LaReau[5]; Carlos E. Astete[3]; Cristina M. Sabliov[3]; Leonardo F. Fraceto[6]; Valdemar L. Tornisielo[1]; Christian O. Dimkpa[4]; Jason C. White[4]

[1]Center of Nuclear Energy in Agriculture, University of São Paulo, Piracicaba, SP 13416-000, Brazil; [2]Department of Plant Pathology & Nematology, Superior School of Agriculture "Luiz de Queiroz", University of São Paulo, Piracicaba, SP 13418-900, Brazil; [3]Biological & Agricultural Engineering, Louisiana State University and LSU Ag Center, Baton Rouge, LA 70808, United States; [4]Department of Analytical Chemistry, The Connecticut Agricultural Experiment Station, New Haven, CT 06511, United States; [5]Department Environmental Science and Forestry, The Connecticut Agricultural Experiment Station, New Haven, CT 06504, United States; [6]Institute of Science and Technology, São Paulo State University (UNESP), Sorocaba, SP 18087-180, Brazil.

*Correspondent author: vanessatakeshita@usp.br and vanessatakeshita@gmail.com

Abstract

Several studies have reported improved weed control and targeted delivery of herbicides by nanocarriers. However, the effects on crops and non-target organisms need to be considered. Here, we investigate the crop and soil health treated with metribuzin in conventional and biodegradable nanoformulations (poly-ε-caprolactone - PCL and lignin-PCL) (both at 480 g a.i. ha^{-1}). Weed control of *Amaranthus retroflexus* by the nanoformulations was also evaluated as a measurement of target delivery. Soybean plants did not show any differences in photosynthetic parameters and a slight oxidative stress with nanoherbicide treatment, with biomass reduction occurred at 60 days after application. The root accumulated metribuzin formulations and translocated to the aerial part for both plant species. The polymeric nanomaterials in the soil mitigated alterations in the bacterial community. Metribuzin formulations, mainly nanoformulations even at low dose (48 g a.i. ha^{-1}) caused severe photosynthetic damage in the weed species, with reduction of chlorophyll content (up to 2.35 time) and electron flow (up to 9.22 times), leading to eventual mortality. MTZ nanoformulations presented a greater efficacy (even in 10-fold less dose) for weed control compared to conventional formulation. These findings suggest that MTZ nanoformulations improve weed control and attenuate the negative effects on crop and soil health, offering an important nano-enabled strategy for sustainable weed management.

Keywords: Nanoherbicide, PCL, lignin, weed control, plant uptake, non-target plant, target plant.

1. Introduction

Pesticides are used to maintain crop production in the face of adverse biotic conditions. Among the pesticides, herbicides are used for weed control, helping to reduce multispecies competition for nutrients, water, and space with food crops. In 2021, herbicides represented almost 49% of the total pesticides used worldwide, corresponding

to 1.8 thousand tons [1]. Use of herbicides has increased exponentially since the development of herbicide-tolerant crops [2,3]. However, current herbicides are hampered by low delivery efficiency, leading to considerable negative environmental impact, as well wasted energy and water inputs [4].

Another significant shortcoming of herbicides is related to their effects on non-target species [5–7]. Schulz et al. [8] studied data on 381 pesticides studied over 25 years and demonstrated notable increase in toxic effects on non-target plants by herbicides. Importantly, nanoformulations of pesticides have demonstrated reductions in environmental risk and non-target effects, while simultaneously having increased efficacy [9–17]. Overall, nanoherbicides have lower toxicity than conventional herbicide formulations, mainly due to the use of nature-inspired nanocarriers such as zein, chitosan, lignin, and alginate [4,11,18–20]. However, a more comprehensive investigation and subsequent analysis is necessary to improve knowledge of nanoformulations for further safe and optimized applications [21]. Studies with non-target plants, beyond weed control assays, are a critical part of these investigations.

Metribuzin is a model herbicide that has been evaluated for delivery by nanocarriers. For example, metribuzin nanoparticles based polycaprolactone (PCL), a flexible biodegradable plastic [22], showed 7.2% higher weed control than conventional metribuzin formulation at recommended dose for field application (480 g a.i. ha^{-1}) and 35.37% at 10-fold recommended dose (48 g a.i. ha^{-1}) [15]. Similar to conventional metribuzin, the same nanoformulation presented low retention and potential mobility in soil, even in different tropical agricultural tropical soils [23]. Also, the authors observed low persistence (~15 d) and no negative effects on soil enzymatic activity (acid phosphatase, β-1,4-glucosidase, and arylsulfatase) in spite of effective weed control of *Ipomoea grandifolia* (480-48 g a.i. ha^{-1}) [24]. Lignin-based nanocarriers have begun to generate interest in other applications but have not been reported yet for metribuzin. Salinas et al. [4] investigated lignin polymeric nanoparticles as a cargo-free nanoplatform and showed a negligible impact on exposed soybean plants, with no biomass reduction and oxidative damage, except for a slight SOD increase at 7 and 14 days after application. Little information on the effects of lignin-based nanoparticles loaded with metribuzin on non-target and target plants, relative to other biodegradable nanocarriers, is available in the literature.

Here, we investigate the uptake and physiological effects of metribuzin formulations (conventional and nanoformulations) on soybean plant as indicators of

ecological safety and crop health. In addition, we assessed the weed control efficacy of the metribuzin in conventional and nanoformulations on *Amaranthus retroflexus*. Importantly, this is the first study examining the uptake, physiological, and photosynthetic effects of metribuzin nanoformulations on target (weed) and non-target (food crop and soil microbial community) species. Notably, the importance of comparisons between biodegradable nanoformulations from different materials were made to better understand their safety and potential use as herbicide nanoformulations.

2. Material and Methods

2.1 Chemicals

Technical grade metribuzin (95% purity) was was kindly provided by the U.S. Food and Drug Administration (FDA). For preparation of nanoparticles, caprylic/capric triglyceride (Myritol 318) was purchased from BASF (BASF Co. Ltd., São Paulo, SP, Brazil), while poly-ε-caprolactone (PCL) (Mn~80,000 Da), polysorbate 80 (Mn~1310 Da), sorbitane monostearate (Mw = 430.63 g mol^{-1}), ε-caprolactone (CL, >99%), and stannous 2-ethyl hexanoate ((Sn(Oct)2) - purity 92.5-100.0%) were purchased from Sigma Aldrich (Sigma-Aldrich, Chem. Co., St. Louis, MO, USA). A alkaline lignin was procured from TCI Inc. (Portland, OR), and rhodamine B (99% purity) was purchased from Avanti Polar Lipids (Avanti Polar Lipids®, Alabaster, Alabama, USA). For the process of fixing slides for microscope analyses, paraformaldehyde (95% purity) was purchased from Sigma Aldrich (Sigma-Aldrich, Chem. Co., St. Louis, MO, USA) and fluoromount (99% purity) was purchased from Thermo Fisher Scientific (Waltham, Massachusetts, USA).

2.2 Synthesis of PCL-lignin polymers

Polymers were synthesized by ring opening polymerization (ROP) of the monomer CL, following a slight modification of a previously reported procedure [25,26] using alkali lignin that was dried in a vacuum oven before synthesis. Briefly, 2 g of alkali lignin was placed in a 250 ml 3-neck round-bottom flask, and then 4 g of CL was added. The mixture was heated and stirred in an oil bath at 130 ˚C. Subsequently, 0.2% (v/v according to CL volume) of $Sn(Oct)_2$ was added as a catalyst. The grafting reaction proceeded for 24 h with constant stirring at 200 rpm under argon flow to create anhydrous

conditions. When the reaction was complete, the solution was precipitated dropwise into 200 ml cold methanol. The supernatant was discarded, and the precipitate was washed five times with cold methanol.

The resulting grafted polymer was then diluted in 200 mL dichloromethane and washed five times with distilled water to remove unreacted lignin. The polymer was then concentrated in a Rotavapor R-300 (Buchi Corporation, New Castle, DE). The resulting solids were frozen at -80 ˚C for 24 h and lyophilized using a freeze dryer (FreeZone Plus 2.5; Labconco, Kansas City, MO) to remove all water and solvents from the polymer. Finally, the PCL-lignin polymer was stored in a desiccator at room temperature for future use. PCL-lignin exhibited a degree of polymerization of 37 as determined by ^{1}H NMR (Fig. S1).

2.3 Preparation and characterization of nanoformulations

Two nanoformulations were prepared as metribuzin herbicide nanocarriers. The poly-ε-caprolactone metribuzin nanoparticles (PCL-MTZ) were prepared based on Takeshita et al. [15] by the nanoprecipitation method, which consists of an organic phase (100 mg of PCL, 200 mg of Myritol, 40 mg of SPAN, and 10 mg of technical-grade MTZ in 30 mL of acetone as a solvent) and an aqueous phase (60 mg of Tween 80 and 30 mL of ultrapure water). The solutions were agitated in magnetic stirrer and mixed under the same conditions. After 20 min, the solvent was removed by rotary evaporation (Buchi R300, Buchi Corporation, New Castle, DE) until 10 mL of final volume (1 mg mL^{-1}).

PCL-lignin MTZ nanoparticles were prepared using an emulsion evaporation method based on Salinas et al. [4] with modifications. The organic phase was prepared by combining 800 mg of PCL-lignin copolymer and 80 mg of metribuzin in 20 mL of dichloromethane and acetone (1:1 *v*/*v*). The aqueous phase was 200 mL water. The phases were mixed by adding the organic phase dropwise to the aqueous phase under magnetic stirring. The emulsion was passed through a microfluidizer (Microfluidizer M-110P, Microfluidics International corporation, Westwood, MA) five times at 30 kpsi. The organic solvent was evaporated out of the solution using a rotavapor for 2 h, followed by the addition of 1000 mg trehalose for cryoprotection. The final formulation was lyophilized (Labconco 2.5 freezone, Labconco Corporation, Kansas City, MO) for 2 days, and was recovered a dark yellow powder (final concentration of 0.0631 mg of MTZ in 1

mg nanoparticles powder). The work solution was prepared considering the same concentration of PCL-MTZ, diluting the PCL-lig-MTZ powder in deionized water, at 1 mg mL^{-1}.

For plant experiments, nanoparticles were prepared by adding technical grade metribuzin (purity of 98%) into the organic phase. For microscope analysis, 100 µL of a fluorescent probe (rhodamine B) was added in the same organic phase to track nanoparticles inside the plant species. The stability of nanoparticles was measured by dynamic light scattering (DLS) technique, evaluating the mean size (hydrodynamic diameter) of particles, polydispersity index (size uniformity of nanoformulation), and zeta potential (surface charge). A dilution of nanoparticle suspension (1:1000, v/v) was prepared and analyzed in triplicate using a Malvern Zetasizer ZS (Malvern Analytical, Westborough, MA), at 25°C.

Transmission electron microscopy (TEM) was carried out on a Hitachi 7800 microscope for morphological characterization of the nanoformulations. To this end, a suspension of the nanoformulation containing uranyl acetate (1%) as a contrast agent was placed on a copper grid. The samples were dried in ambient air for 24 h prior to analysis.

2.4 Soil collection and plant material

Soil was collected from Lockwood Farm, Hamden CT, United States (41°24'29.3"N 72°54'12.6"W). The soil, a sandy loam, was collected at a depth of (0-0.20 cm), from a site with no record of metribuzin application. All soil characteristics are described in Table S1. The soil samples were sieved (2 mm) and mixed with 20% of Pro-mix® commercial substrate, and the mesocosm and weed plants experiment units were filled with 800 g and 250 g of soil, respectively.

For the plant experiments, soybean (*Glycine max* cv. Karikachi) seeds were purchased from Johnny's Seeds (Winslow, Maine, USA). For the weed experiments, *Amaranthus retroflexus* plants were collected from Lockwood Farm, Hamden, CT - United States (41°24'29.4"N 72°54'14.2"W) and stored in paper bags until the beginning of sowing. All plants developed in a greenhouse for 60 days (23-17 °C) with a 10 to 13 h photoperiod.

2.5 Non-target plant assay

Pots containing soybean plants was prepared as a non-target assay. Pots of 1 L capacity were filled with 800 g of soil mix. Before sowing, water capacity was tested in

the potted soil to avoid leaching of formulations outside the pots, and 15 mL day^{-1} was established as simulated precipitation. Five soybean seeds were sown in each pot 24 h before treatment application. The experimental design was randomized, with four treatments (water, MTZ non-encapsulated, PCL-MTZ, and PCL-lig-MTZ), and six replicates. All treatments were applied with the distribution of 1 mL of working solutions containing water and the herbicide active ingredient directly, or embedded in the nanoformulations, prepared at 480 a.i. g h^{-1} dose, considering the pot area (10 cm^2), MTZ mass, and final concentration of nanoformulations. Plants were cultivated in the greenhouse for 60 days after application (DAA). The evaluation time points were 15, 30, 45, and 60 DAA. At each time point, photosynthetic parameters were acquired by non-destructive measurement as described below. Oxidative stress parameters, biomass, length, and metribuzin quantification were obtained with destructive samples. Soil samples were collected for microbial analysis and metribuzin quantification.

2.5.1 Analysis of photosynthetic parameters

A portable PhotosynQ (PHOTOSYNQ INC., East Lansing, MI, USA) was used to measure photosynthetic parameters, including PhiNO, PhiNPQ, Phi2, Relative chlorophyll, and linear electron flow (LEF), a once per week for 60 days. A fixed location was established in the greenhouse for all days of photosynthetic parameter measurements to avoid significant variations in light.

2.5.2 Oxidative stress analysis

The effects of nanoherbicides on oxidative stress were analyzed through the quantification of malondialdehyde (MDA), ascorbate peroxidase (APX), catalase (CAT), and superoxide dismutase (SOD). For APX, CAT, and SOD an extraction method based on [27] and [28] was carried out. For this analysis, 0.2 g of plant tissue (depending on if aerial part or root tissue) for each enzyme (0.6 g in total) was vigorously mixed with 6 mL of 25 mM potassium phosphate buffer solution (KH_2PO_4, pH 7.4) using a high-speed homogenizer (12,000 g for 2 min). Samples were centrifuged at 5,000 g and 4°C for 15 minutes. Then, 1.5 mL of supernatant was frozen in liquid nitrogen and stored at -80°C until analyses. An extraction method based on [29] was used for MDA. A mixture of 0.2 g of plant tissue (aerial part or root) with 0.1% (w/v) trichloroacetic acid (TCA) was homogenized vigorously using a high-speed homogenizer (5,000 rpm for 2 min). The

same centrifugation and supernatant collection performed for other enzymes was applied to MDA.

APX activity was determined by decreased absorbance of the H_2O_2 method [30]. For measurements, 40 µL of the extract sample was mixed with 228 µL of 0.5 mM ascorbic acid and 532 µL of 0.4 mM H_2O_2. The absorbance of the reactions was measured in a 96-well plate, in triplicate (200 µL each replicate), at 290 nm with 2 min total run time, by UV–vis spectrophotometer (Molecular Devices, SpectraMax M2). A calibration curve of H_2O_2 (10-0.3 mM) was established and used for quantitation.

CAT activity was determined according to Medina-Velo et al. [30] by measuring the decrease in absorbance of H_2O_2. For measurements, 40 µL of the extract sample was mixed with 760 µL of 10 mM H_2O_2. The sample absorbance was measured in a 96-well plate, in triplicate (200 µL each replicate), at 240 nm with 3 min total run time, by UV–vis spectrophotometer. The same calibration curve for APX was used to calculate the CAT activity in the plant samples.

To determine SOD activity, a method involving the photochemical reduction of nitroblue tetrazolium (NBT) was used [27,30]. A buffer mix solution was prepared with 500 µM NBT, 78 mM L-methionine, 1.5 mM EDTA, and 100 mM potassium phosphate buffer (pH 7.8). Thirteen µL of plant extract was mixed with 707 µL buffer solution and 80 µL of 0.02 mM riboflavin solution. The mixture was transferred to a 96-well plate and then illuminated for 15 min in a box with a compact fluorescent light and the absorbance measurements were made by UV–vis spectrophotometer (560 nm). Inhibition of NBT was determined by comparing samples without plant extracts (illuminated and non-illuminated). Units of SOD activity were defined as the amount of enzyme activity causing to a 50% reduction in NBT concentration.

For MDA determination, the thiobarbituric acid reactive substances (TBARS) method was used [31]. A mixture of 160 µL of plant extract, 400 µL of 2% trichloroacetic acid (TCA), and 400 µL of 0.5 % thiobarbituric acid (TBA) was heated at 95°C for 30 min and then immediately cooled on ice until R.T. The absorbance of MDA was measured in a 96-well plate, in triplicate (200 µL each replicate), at 532-600 nm, by UV–vis spectrophotometer. The final MDA concentration was calculated based on Lambert−Beer's equation (extinction coefficient of MDA is 155 mM cm^{-1}).

2.5.3 Plant physiological parameters and soil collection

Soil samples were collected from each pot (n=6) at 2 soil points (in all soil depths), totaling ~3 g per pot, for metribuzin quantification by LC-MS. The mass and length of the soybean were measured at 15, 30, 45, and 60 DAA through destructive sampling. All samples were stored at -20°C until plant (oxidative stress and metribuzin quantification) and soil analysis (metribuzin quantification) was completed.

2.5.4 Metribuzin quantification

Metribuzin extractions were carried out using the QuEChERS method, based on Hazra et al. [32]. Approximately 1 g of plant tissue (depending on if aerial part or root tissue) or soil was added in 50 mL conical tubes, the volume was adjusted to 15 mL with deionized water, and then 10 mL of acetonitrile was added. Samples were homogenized in a high-speed homogenizer for 30 seconds at 12,000 g. For the salts of amendment, 1 g of NaOAc and 4 g of $MgSO_4$ were added to the solution, followed by homogenization and centrifugation for 5 min at 12,000 g at each step. Ten mL of supernatant was collected and transferred to 15 mL conical tubes with clean-up salts (0.15 g of PSA sorbent, 0.45 g of anhydrous $MgSO_4$, and 0.05 g of C_{18}). The mixture was homogenized and centrifuged under the same conditions described above. One mL of the supernatant was collected, concentrated by evaporation (TurboVap® LV, Biotage), and resuspended in 100 µL of acetonitrile. Samples were placed in chromatography vials and stored at -20 °C until analysis.

Samples were analyzed by liquid chromatography-mass spectrometry using a Dionex UltiMate 3000 liquid chromatograph equipped with an Agilent SB-C_{18}-RRHD-2.1 mm × 150 mm column packed with 1.8 µm particles (Agilent Technologies, Santa Clara, CA, USA) coupled to a Thermo Q Exactive high-resolution mass spectrometer (Thermo Fisher Scientific, Waltham, MA, USA). Mobile phases were 0.1% formic acid in water (A) and 0.1 % formic acid in acetonitrile (B). Initial mobile phase composition was 5% B ramped to 95% B over 12 min at a 0.2 mL min^{-1} flow rate. Calibration curves were obtained by making a series of metribuzin standards at different concentrations. An external standard calibration curve was used with continuing calibration verification injections performed at the beginning, during, and at the end of each analytical batch. For quality assurance, every analytical run contained a reagent blank and continuing calibration verification (CCV) samples at regular intervals.

2.5.5 Soil microbial diversity

Microbial diversity in the soil was analyzed according to [33]. Total DNA was extracted from 0.25 g of soil from the resulting pellet using the DNeasy PowerSoil kit (Qiagen). DNA extractions were verified by gel electrophoresis in a 1% agar gel. Bacterial 16S rRNA genes were amplified with the primer pair 515F (GTGYCAGCMGCCGCGGTAA) and 806R (GGACTACNVGGGTWTCTAAT) with dual indexing of the Illumina I5 and I7 tags [34]. Extracts were amplified with 10 μL Platinum SuperFi II DNA polymerase (Invitrogen), which also included 7.5 μM both the mPNA and pPNA peptide nucleic acid (PNA) clamps (mPNA, GGCAAGTGTTCTTCGGA; pPNA, GGCTCAACCCTGGACAG) to block the amplification of host plant mitochondria and plastid rRNA genes, respectively [35,36]. PCR conditions consisted of 94 °C for 2 min followed by 30 cycles of 94 °C for 15 s, 60 °C for 15 s, 68 °C for 15 s, and 4 °C for an infinite hold. The resulting amplification products were verified by gel electrophoresis, and cleaning and normalization of individual PCR products was performed with a SequalPrep normalization plate (Invitrogen). The normalized PCR amplicons were mixed, and the quantity and quality of the DNA pool were verified using an Agilent TapeStation. The resulting 16S rRNA gene amplicons were sequenced on the Illumina MiSeq 100 system employing 250 base pair chemistry at the Yale Center for Genome Analysis (YCGA, New Haven, CT, USA).

16S rRNA gene sequences were initially processed using the Mothur software package (v. 1.44.2) [37]. Quality filtering is selected for sequences of at least 250 bp in length. Chimeric sequences were identified with the VSEARCH algorithm as implemented in Mothur (Rognes et al., 2016), using the most abundant sequences as a reference for chimera detection. All putative chimeric sequences were removed from the data sets. The 16S rRNA sequences were classified against the SILVA v138 reference database [38] using the RDP naive Bayesian classifier as implemented in Mothur [39], and sequences identified as belonging to eukaryotes or that were unclassified were removed. The resulting sets of sequences were assigned to amplicon sequence variants, employing a 100% sequence similarity threshold.

2.6 Target plant assay

2.6.1 Weed control assay

In the weed control assay, *A. retroflexus* seeds were sown (~10 g) in 250 mL soil mix pots 24 h before treatment application (treatment in pre-emergency of weed plants). The experimental design was randomized, with 8 treatments (Table 1), and 4 replicates.

Dose calculations were made considering the pot area (45 cm²) and MTZ concentration in each formulation, using the technical grade metribuzin. The treatments were applied using a liquid working solution over the soil (1 mL) with a pipet. Evaluations were conducted at 7, 14, and 21 DAA with pot harvest and dry biomass determination after 48 h in a ventilated oven (60 ºC).

Table 1. Pre-emergent treatments applied for *Amaranthus retroflexus* in the weed control assay.

Treatments	Dose (g a.i. ha^{-1})
Water (control)	---
MTZ (positive control)	480*
PCL-MTZ (full-dose)	480
PCL-MTZ (half-dose)	240
PCL-MTZ (1/10-dose)	48
PCL-lig-MTZ (full-dose)	480
PCL-lig-MTZ (half-dose)	240
PCL-lig-MTZ (1/10-dose)	48

*Based on commercial recommendation (Sencor® 480, Bayer CropScience).

2.6.2 Assessing herbicide uptake by fluorescence microscope analysis

To determine metribuzin uptake and translocation, seeds were sown on trays, and then seedlings were transplanted 15 days after germination to the experimental pots (250 mL pots). Pots with transplanted *A. retroflexus* (one plant per pot) received treatments after 3-4 fully expanded leaves. The experimental design was completely randomized, with a 2 x 3 factorial arrangement, where 2 are PCL-MTZ and PCL-lig-MTZ, both with rhodamine B encapsulated as a fluorescent probe, and 3 evaluation days (1, 3, and 5 days after application), with 5 replicates. The samples were separated into fully expanded newest leaf and root tissue. The sampling was carried out in a dark room to avoid the degradation of the rhodamine B probe.

The sample preparation method was based on Preisler et al. [40]. A sterile blade was used, and ethanol sterilization was performed after each cutting sequence. Squares (1 cm²) in the middle leaves were removed, fixed, and placed in slides as described below. For tissue fixation, samples were placed in 50 mL conical tubes containing 10 mL of 4% paraformaldehyde solution and shaken at 140 rpm for 4 h at 22ºC. Samples were then transferred to new tubes containing a phosphate buffer solution (PBS, pH 7.0), and subjected to 10-minute shaking under the same conditions as the previous step. The samples were stored in 50 mL conical tubes containing 10 mL of azide PBS and

refrigerated in the dark. Slides of plant samples were prepared with 100 µL of fluoromount. Images were obtained in a Zeiss Axio Imager M1 fluorescence microscope with excitation ranging from 538 to 562 nm and emission ranging from 570 to 640 nm. After collecting all images, the Zen 3.7 (Zeiss Zen Lite) software was used for fluorescence quantification and data was expressed in terms of fluorescence intensity (FI).

2.6.3 Analysis of herbicide uptake and effects of nanoformulations on photosynthesis in weed plants

Weed plants in pots received the same treatments as described in Section 2.4.2 to quantify metribuzin in plant parts (aerial part and roots) and the photosynthetic parameters were assessed, as described for soybean plants. The extraction method and LC-MS analysis were carried out according to Section 2.3.4. Measurements were carried out at 1, 3, 5, and 7 DAA by destructive sampling. These data were used to support the uptake of nanoformulations analyzed by fluorescence microscopy and the analogous weed control assay.

2.7 Statistical analysis

The datasets for the photosynthetic parameters (PhiNO, PhiNPQ, Phi2, Relative chlorophyll, and LEF), oxidative stress indicators (MDA, APX, CAT, and SOD), physiological parameters (mass and length), concentration of metribuzin in soil and plants were subjected to variance analysis (ANOVA). When significant according to an F's test ($F<0,05$) and to ANOVA assumptions (homoscedasticity and homogeneity of variances) ($p>0,05$), data was analyzed by to the Tukey's test ($p>0,05$, $n=4$). Weed control data was also subjected to Dunn's test, by Kruskal-Wallis multiple comparison test, to indicate the difference between the metribuzin treatments and control treatment with water. The figures were plotted using Origin® 2020 (Version 9.7.0.185, OriginLab Corporation, Northampton, MA, USA). For the soil microorganism diversity effects evaluation, the Mothur output files were imported into the phyloseq R package for descriptive and statistical analyses [41]. Detrended correspondence analysis was performed with Bray-Curtis similarities calculated between samples. Significant differences in clustering were determined with the adonis2 function of the vegan R package [42]. Biomarkers distinguishing the different treatments were identified with the linear discriminant analysis (LDA) effect size (LEfSe) method as implemented in the microbiome Marker R package [43,44].

3. Results and discussion

3.1 Nanoformulations characteristics

The synthesized PCL-MTZ and PCL-lig-MTZ nanoformulations presented hydrodynamic sizes of 265.83 ± 1.79 nm and 178.23 ± 0.26 nm, respectively (Table S2). PCL-MTZ nanoparticles had a PDI of 0.17 ± 0.05 while PCL-lig-MTZ had a PDI of 0.34 ± 0.03. The charges were negative, -27.33 ± 0.03 mV for PCL-MTZ and -42.27 ± 0.07 mV for PCL-lig-MTZ. Both nanoparticles are thus considered homogeneous nanoformulations [15,20,45]. A spherical shape was observed for both metribuzin nanoformulations (Fig. S2a and S2b), which was expected for PCL nanoparticles based on prior studies [15,18,45]. The PCL-MTZ presented high encapsulation efficiency (74.8% ± 0.5) and stability over time (120 days), with a release of 70% in 24 h that is associated with the diffusion of herbicide by swelling and relaxation of the polymer matrix [15]. PCL-lig-MTZ presented 96% of encapsulation efficiency, with 31.67% of agrochemical in the first 24 h [26]. The PCL-MTZ has a 1.82% loading capacity, while PCL-lig-MTZ has 4.08% (estimated with the previous data available in the literature) [15,26]. In summary, all measured characteristics indicate significant potential of the nanoformulations to encapsulate and deliver metribuzin to plants.

3.2 Pot studies

3.2.1 Non-target plant photosynthetic effects

The photosynthetic parameters of soybean exposed to MTZ formulations are presented in Figure 1. The PhiNO, PhiNPQ, and Phi2 indicated a similar effect of nanoencapsulated MTZ in soybean plants at 60 DAA (Fig. 1a, b, and c). All of these parameters are related to energy losses in the photosynthetic process; there was limited impact of the nanoformulations, followed by complete recovery by the final time point. The relative chlorophyll conten was not affected by treatment across all evaluation days (Fig. 1d), except for PCL-MTZ at 60 DAA. The linear electron flow (LEF) was not negatively affected by treatment (Fig. 1e); in fact, values were significantly increased in after 45 DAA in the presence of the nanoformulations, being 1.29 times higher than in MTZ-treated plants.

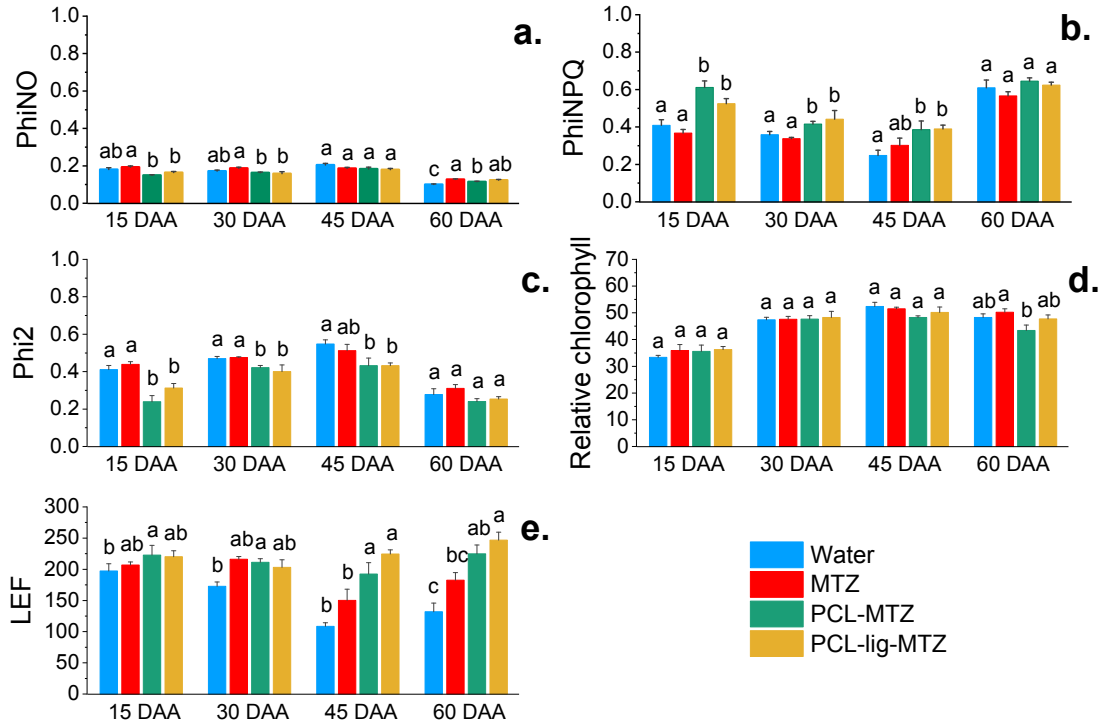

Figure 1. Photosynthetic parameters (PhiNO, PhiNPQ, Phi2, Relative chlorophyll, and LEF) of soybean plants at 15, 30, 45, and 60 days after application of metribuzin non-encapsulated (MTZ) and nanoencapsulated in two formulations (PCL-MTZ and PCL-lig-MTZ at 480 g a.i. ha^{-1}). Bars represent the mean and standard error mean. Different lowercase letters represent statistical differences between treatments on each evaluation day, on each parameter by Tukey's test (p<0.05; n=6).

The PhiNO, PhiNPQ, and Phi2 parameters are represented by unit values corresponding to the yields for dissipative processes of the energy absorbed by the photosystem II. The Phi2 is the photochemistry yield from PSII, and PhiNPQ is the non-photochemical quenching of chlorophyll fluorescence, both of which occur in proteins that comprise the antenna system for PSII [46]. PhiNO is another non-photochemical yield energy dissipation endpoint, corresponding to absorbed light that is not used for photochemistry or dissipated by NPQ (non-photochemical fluorescence quenching) [47]. For Phi2, until 45 DAA soybean plants treated with PCL-MTZ and PCL-lignin-MTZ showed less photochemistry yield than water and MTZ-treated plants. We observed an inverse effect for PhiNPQ. The activity of NPQ can be increased as a response to reactive oxygen species generation [48].

Importantly, MTZ is a known photosynthesis II inhibitor, and the effect of the non-encapsulated MTZ was similar to the water treatment in most evaluations, indicating a metribuzin herbicide tolerance level of this soybean cultivar. Gabr et al. [NO_PRINTED_FORM] [49] indicated that even with inhibitory effects on the biosynthesis of

pigments (chlorophyll), the chlorophyll ratio *a*/*b* was not affected 60 days after metribuzin application in soybean. A number of strategies for the metabolism or differential distribution of metribuzin in soybean cultivars have been described in the literature [50–52], indicating non-negative effects in plants even when associated with nanoparticles. The LEF data showed gains in energy throughout the photosystem. Also, biodegradable nanoparticles have been shown to increase photosynthesis in plants by a number of different mechanisms, including an increase in light absorption, augmentation of protein and chlorophyll content in plants, or other unknown processes [53]. Process related to carbon metabolism could also be involved. Therefore, the MTZ detoxification and the presence of nanoscale carbon structures can contribute to photosynthetic processes and carbohydrate production.

3.2.3 Non-target plant oxidative stress

Slight oxidative damage was observed with enzyme activity over time (Fig. 2). For SOD from roots and aerial part, some differences were found between treatments within the first 15 days of evaluation; however, herbicides treatment did not show a higher antioxidant effect than the treatment with water after 30 DAA (Fig. 2a). For APX and CAT, an increase over time was observed in aerial parts (Fig 2b and c), with no oxidative damage presented at 60 DAA. For MDA, the enzyme activity in the roots was similar after 45 DAA and in the aerial part, a slight effect for PCL-lig-MTZ was detected overtime. However, the MTZ treatments did not cause significant damage to the exposed soybean plants.

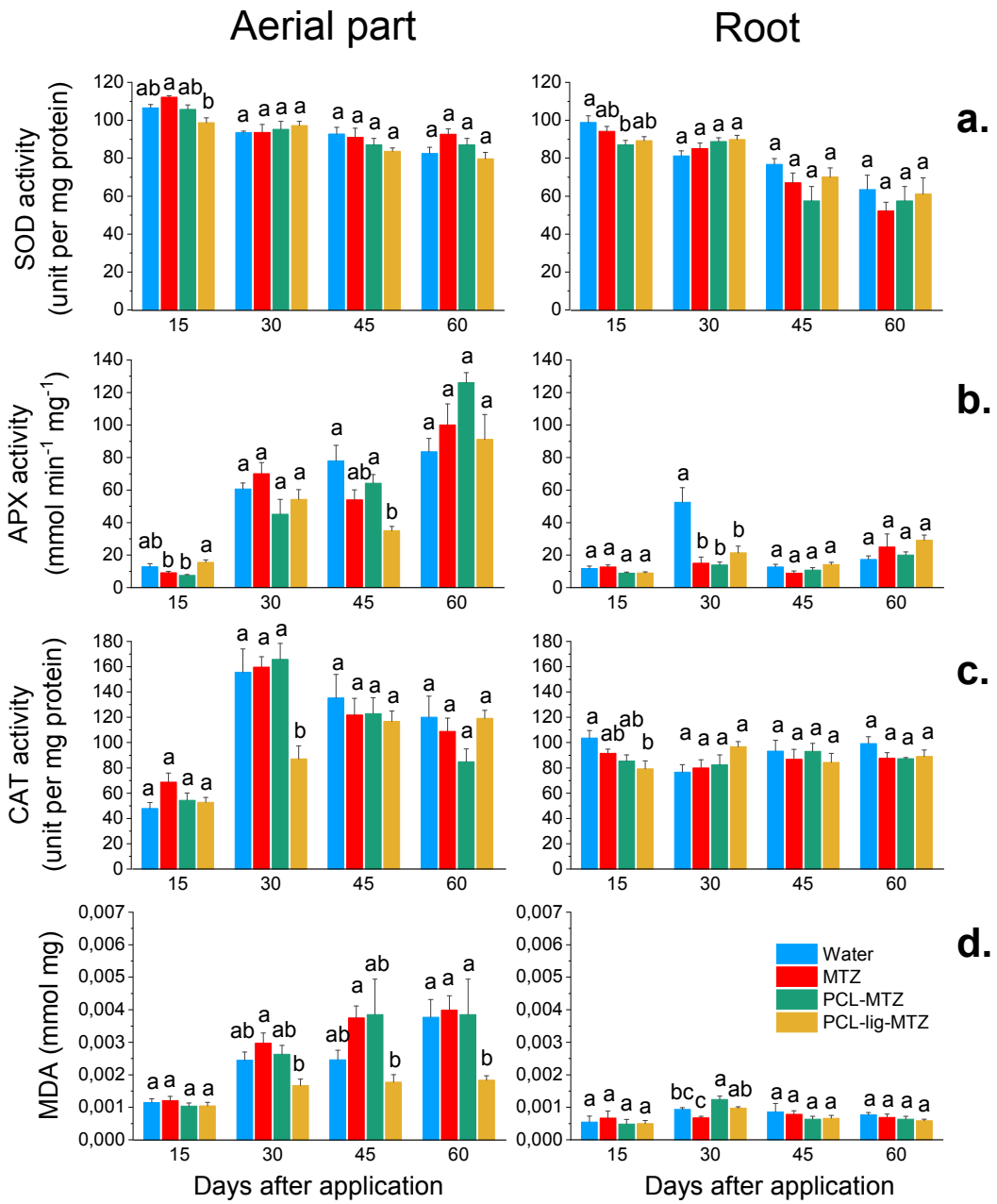

Figure 2. Oxidative stress enzyme activities (**a,** APX, **b,** CAT, **c,** MDA, and **d,** SOD) of soybean plants at 15, 30, 45, and 60 days after application of metribuzin non-encapsulated (MTZ) and nanoencapsulated in two formulations (PCL-MTZ and PCL-lig-MTZ at 480 g a.i. ha^{-1}). The left column indicate enzyme activity in the aerial tissues and the right column is root data. Bars represent the mean and standard error mean. Different lowercase letters represent statistical differences between treatments on each evaluation day, on each enzyme, by Tukey's test (p<0.05; n=6).

SOD, APX, and CAT are enzymes involved in mitigating reactive oxygen species and hydrogen peroxide stress in plants [54]. This data indicates that the nanoformulations were causing slight significant oxidative stress or associated damage in the exposed soybean plants. Nakasato et al. [55] showed that phytotoxicity was highly nanomaterial

specific, as chitosan/tripolyphosphate presented negative effects on *Zea mays*, *Brassica rapa*, and *Pisum sativum* plants compared to solid lipid nanoparticles. Kacsó et al. [NO_PRINTED_FORM] [56] observed little or no effect of zein and lignin-based nanoparticles on soybean seed viability and plant growth. Also, PCL-based nanoparticles did not cause adverse effects, such as lipid peroxidation, in maize [57].

MDA activity in the aerial tissues of plants treated with PCL-lig-MTZ showed lower levels compared to all other treatments at 30 DAA (Fig. 3d), in spite of the innate increase in enzyme activity during the growth period. As noted above, MDA activity is a bioindicator of lipid peroxidation [31]; plant cellular membrane leakage, necrosis, and biomass loss can be symptoms of this process. Notably, only at 60 DAA did plants that received PCL-MTZ and PCL-lig-MTZ formulations present mass loss (described in the section below at 60 DAA). The occurrence of lipid peroxidation can be an indicator of damage, but no such impacts were noted upon exposure to the nanoformulations. Importantly, MDA quantitation must be interpreted as a marker of lipid peroxidation with caution due to interferences in the absorbance signals of the enzyme by other carbohydrates and anthocyanins, with a possible overestimation of the values obtained by the TBA method [58]. Nevertheless, our results showed little evidence of harmful oxidative effects associated with MTZ treatment in soybean. Importantly, despite the slight oxidative stress observed, the MTZ nanoformulations offered an efficient weed control alternative, mainly due to the possibility of the active ingredient reduction.

3.2.4 Non-target plant physiological responses

Plant mass and length were measured at 60 DAA (Fig 3a and b). No fresh biomass reduction was observed in roots over the experimental period and for the shoots until 45 DAA. Despite the absence of oxidative effects on the plants, the nanoformulations reduced of the soybean plant mass by ~32% at 60 DAA compared to the water and MTZ treatment. Crop plant mass reduction is not frequently reported for nanoherbicides [11,57]; nevertheless, the active ingredient rate of application can be reduced (as demonstrated further in section 3.4.1) and the associated risks for the crop can be reduced. Importantly, this possibility in dose reduction and the mass decline of soybean plants at 60 days evidenced the herbicide delivery enhancement, as a function of nanocarriers.

In our greenhouse assay, the pod mass was only reduced by PCL-lig-MTZ (1.57 times less compared with other treatments' mean) (Fig. 3e); however, a field studies to confirm these findings are necessary. No length alterations were evident at 60 DAA as a

function of treatment with metribuzin encapsulated and non-encapsulated formulations, again highlighting the tolerance of this cultivar (Fig. 3b and d).

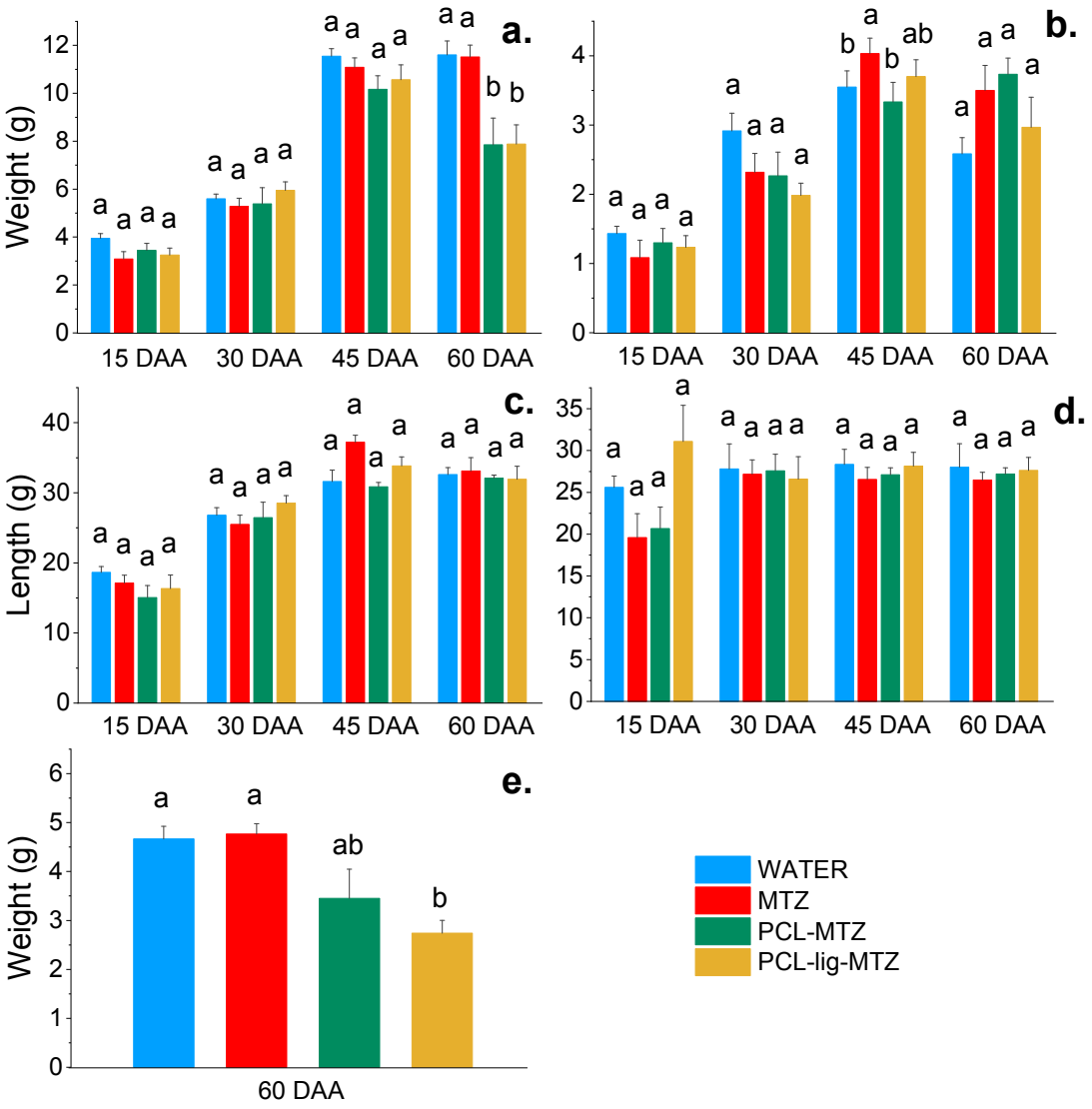

Figure 3. Physiological parameters of soybean plants at 15, 30, 45, and 60 days after application (DAA) of metribuzin non-encapsulated (MTZ) and nanoencapsulated in two formulations (PCL-MTZ and PCL-lig-MTZ at 480 g a.i. ha^{-1}). Fresh mass of aerial part (**a**) and root (**b**) of soybean plants. Length of soybean plants' shoots (**c**) and roots (**d**). Fresh mass of pods (**e**) of soybean plants at 60 DAA. Bars represent the mean and standard error mean. Lowercase letter different represents statistical differences between treatments in each evaluation day, for each parameter, by Tukey's test (p<0.05; n=6).

Although there was no observed photosynthetic and oxidative damage, field studies are needed to ensure the safe application of these nanoformulation so as to understand if the observed biomass reductions may affect over plant growth and yield (Fig. 3e). [11] observed no significant mass reduction in mustard plants treated with PCL

nanoparticles that carried an atrazine cargo (2000-200 g a.i. ha^{-1}). Similarly, Preisler et al. [NO_PRINTED_FORM] [59] observed an increase in the short-term residual effect of atrazine that was loaded in PCL nanoparticles, but recovery from the phytotoxicity on soybeans was evident at 60 DAA. In general, polymeric nanoparticles offer greater safety for crop plants, increase growth and plant protection, and reduce the negative environmental effects associated with pesticide use [60–62]. However, only limited field studies with herbicide nanocarriers have been carried out to date (e.g.[11,24]).

3.2.5 Metribuzin uptake in soybean treated with nanoscale and conventional formulations

Soybean plants exposed to MTZ formulations were analyzed by LC-MS for MTZ concentrations in shoot and root tissues, as well as in the post-harvest soil (Fig. 4). Absorption of MTZ from the polymeric nanoformulations was similar to that of the conventional MTZ (<13 ng g^{-1}) in the shoots (Fig. 4a). In the roots, the values were similar across the treatments but were low (< 4 ng g^{-1}), with some replicates below the detection limit. This indicates significant translocation to the shoot (Fig. 4b). Similar results were observed in the soil, with limitations in detection samples of herbicide at the final time point (Fig. 4c). Takeshita et al. [15] showed that the half-life of MTZ-loaded in polymeric nanoparticles (PCL) was not affected by encapsulation and was similar to that of conventional MTZ (~15 days) in different soils. Therefore, in our study, the level of MTZ in the soil was not found over 60 DAA. In general, non-target plants, even with root absorption and shoot translocation of MTZ, were healthy (no alterations in photosynthetic parameters and no oxidative stress) after herbicide exposure.

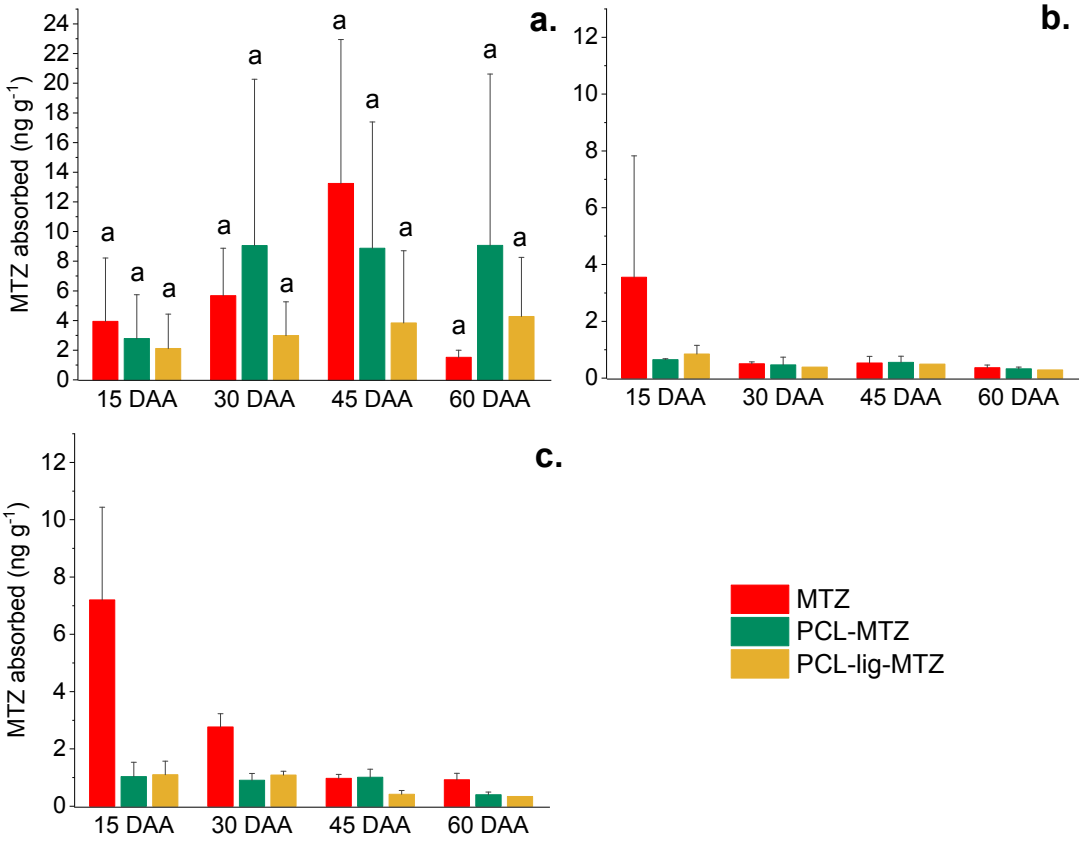

Figure 4. Metribuzin content in soybean plants and soil at 15, 30, 45, and 60 days after application (DAA) of metribuzin non-encapsulated (MTZ) and nanoencapsulated in two formulations (PCL-MTZ and PCL-lig-MTZ at 480 g a.i. ha^{-1}). Amount in shoots (**a**), roots (**b**), and soil (**c**). Bars represent the mean and standard error mean. Different lowercase letters represent statistical differences by Tukey's test between treatments on each evaluation day (p<0.05; n=3). The absence of a value indicates that the analysis of variance and Tukey's test are not suitable, considering the number of samples below the adopted detection limit of MTZ quantification (<6 ng g^{-1}).

3.2.6 Soil microbial community response

To document the response of the rhizosphere bacteria to treatment, 16S rRNA gene sequencing was performed. First, we investigated bacterial diversity. The number of ASVs (amplicon sequence variants) recovered ranged from ca. 9,000 to 13,000 in the initial samples, with the lowest diversity in the water controls. This may be due to additional ASVs being brought in with the treatments as they were not sterile on amendment (Fig. 5a). However, by 60 days, this temporary effect was gone as there were no significant differences in ASVs between treatments. Thus, this data indicated that the taxonomic diversity of the rhizosphere bacteria was generally resilient to these treatments.

The Shannon's diversity index was also evaluated, and this endpoint captures both species diversity and evenness (Fig. 5b). In the initial samples, there were generally no substantial impacts of the treatments on diversity, although PCL-MTZ did have significantly higher diversity ($p = 0.045$). However, after 60 days, the MTZ treatment exhibited significantly lower diversity than the other treatments ($p < 0.001$). These findings suggest that MTZ induced an alteration in the bacterial rhizosphere community, and that importantly, this impact was potentially mitigated by the presence of polymeric material carriers.

Detrended correspondence analysis was performed to characterize variations in community composition. The most influential factor driving community dissimilarities was sampling time, as the initial samples were distinctly separated from the 60-day samples (Fig. 5c). This clustering pattern was highly significant (PERMANOVA $p < 0.001$), these differences were considerably smaller in magnitude compared to the changes observed as a function of time (i.e., throughout plant development).

Last, linear discriminant analysis effect size (LEfSe) was used to identify taxonomic biomarkers associated with the different treatments. Interestingly, only one taxon, the phylum *Acidobacteria*, showed enrichment in the water control samples (Fig 5d). This indicates that these bacteria were particularly susceptible to the herbicide treatments, as their abundance appeared to decrease upon herbicide application. In contrast, two taxa, the family *Sphingomonadaceae* and genus *Burkholderia*, were significantly enriched in the MTZ treatment. Notably, both taxa have been previously reported to possess herbicide degradation capabilities in soil [63–67]. Importantly, we did not observe any taxa that served as biomarkers for the biodegradable polymeric materials, suggesting that the community changes associated with these materials were relatively minor.

Taken together, these findings provide evidence that MTZ treatment caused a significant modification in the rhizosphere bacterial community, leading to a reduction in diversity and the enrichment of bacterial taxa capable of herbicide degradation. Conversely, the incorporation of polymeric substances appeared to mitigate these alterations in the bacterial community. The soil interaction or release rate of pesticides from nanoparticles can interfere in the active ingredients rate that the microbial community is exposed [68]. However, these parameters were not evaluated here. Some authors observed that nanopesticides can present negative impact under soil microbial community (relative abundance and diversity), such as for azoystrobin, diuron, and

atrazine nanoformulations, related to toxicity of pesticide and long-term exposure [69–71]. Nevertheless, when associated pesticides with biodegradable/natural nanoparticles or matrix these effects are reduced due active ingredient protection and low application-rate (slow release) as reported by Prudnikova et al. [72] and Takehsita et al. [15]. As well as providing safety for other non-target organisms [73,74]. This suggests that the addition of polymeric materials played a beneficial role in preserving the composition and functionality of the rhizosphere under the influence of the MTZ treatment.

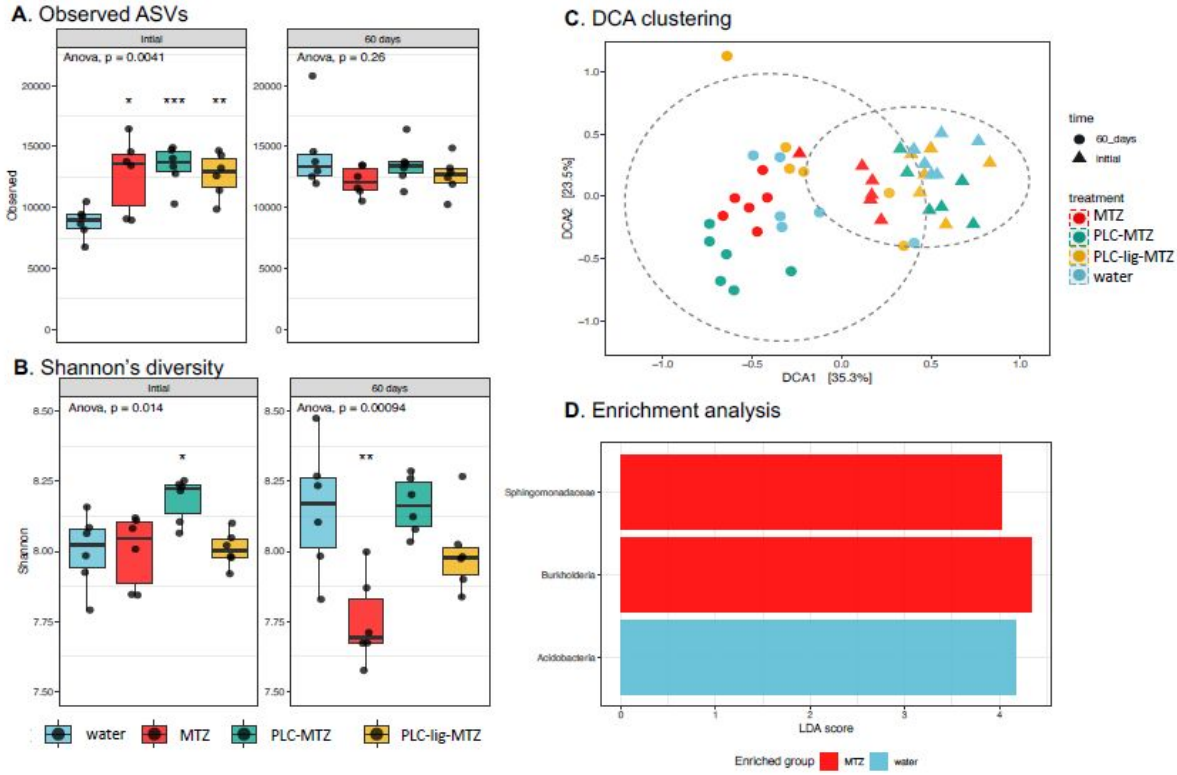

Figure 5. Soil microbial community response 15 and 60 days after application of metribuzin non-encapsulated (MTZ) and nanoencapsulated in two formulations (PCL-MTZ and PCL-lig-MTZ at 480 g a.i. ha^{-1}). Alpha diversity of bacterial communities **a,** Observed ASVs (amplicon sequence variants). **b,** Shannon's diversity index. Significant differences between means were identified by an ANOVA test with the p-value of the test indicated (n=6). The asteric represents the results of a pairwise post-hoc t-test with water as the reference level. P-values: *>0.05, **>0.01, ***>0.001. **c,** Detrended correspondence ordination analysis of bacterial 16S rRNA gene ASVs clustered by sample. Distances were calculated with the Bray-Curtis similarity metric. Ellipses denote the 95% confidence level of datasets grouped by sampling time. The value of the axes indicates the percent variation explained by the respective axis. **d,** LEfSe analysis to identify biomarker taxa. Only categories meeting a log-linear discriminant analysis (LDA) significant threshold >4 are shown. Bars are colored by the treatment in which the genera were enriched as indicated in the legend.

3.4 Weed plant response as a target organism

3.4.1 Weed control

Effective control of *A. retroflexus* was observed in both metribuzin formulation-treated plants, demonstrating effective MTZ delivery by the nanoformulations (Tab. 2). At 7 DAA, MTZ caused a plant biomass reduction of 81.03 ± 14.16 % (480 g a.i. ha^{-1}). For the nanoformulations applied at the full-dose the biomass decrease was 58.62 ± 9.12 % and 44.83 ± 18.03 %, respectively for PCL-MTZ and PCL-lig-MTZ; however, at low doses (48 g a.i. ha^{-1}) the weed control was 82.76 ± 2.82 % for PCL-MTZ and 67.24 ± 13.39 % for PCL-lig-MTZ. After 14 and 21 DAA, the biomass reduction was equal between the doses (recommended, half, and 10 times lower) for both nanoformulations. At 14 DAA, all doses exerted significant weed control (>80%), with e PCL-MTZ at full- and half doses and PCL-lig-MTZ at the full-dose being the most effective. At 21 DAA, both nanoformulations (at full and half doses) and MTZ had exerted 100% mortality. Thus, it is clear that the nanoformulations could control *A. retroflexus* to a greater extent than MTZ, yielding equivalent efficacy at a half-dose of 240 g i.a. ha^{-1}.

Table 2. Dry mass of *Amaranthus retroflexus* at 7, 14, and 21 days after application (DAA) of metribuzin non-encapsulated (MTZ) and nanoencapsulated in two formulations (PCL-MTZ and PCL-lig-MTZ) in full-dose (480 g a.i. ha^{-1}), half-dose (240 g a.i. ha^{-1}), and 1/10-dose (48 g a.i. ha^{-1}).

Treatments	Fresh mass (mg)		
	7 DAA	14 DAA	21 DAA
Water	14.50±4.33[a]	64.00±6.22	236.49±73.09
MTZ (480 g a.i. ha^{-1})	2.75±2.10	0.28±0.28	0.28±0.28
PCL-MTZ (480 g a.i. ha^{-1})	2.50±0.87	0.00±0.00*	0.00±0.00*
PCL-MTZ (240 g a.i. ha^{-1})	1.00±0.41	0.00±0.00*	0.00±0.00*
PCL-MTZ (48 g a.i. ha^{-1})	9.75±3.90	0.75±0.48	32.77±16.25
PCL-lig-MTZ (480 g a.i. ha^{-1})	4.75±1.80	0.00±0.00*	0.00±0.00*
PCL-lig-MTZ (240 g a.i. ha^{-1})	6.50±2.75	0.15±0.15	0.00±0.00*
PCL-lig-MTZ (48 g a.i. ha^{-1})	8.00±2.61	0.25±0.25	9.50±9.50

[a]Mean ± standard error (n=4).
*Indicate a difference between the metribuzin treatments and control treatment with water by Dunn, by Kruskal-Wallis multiple comparison test.

Being able to reduce the active ingredient amount applied for weed control is a significant advantage of nanoherbicides for sustainable agriculture. A number of studies have reported that polymer-based nanoparticles have the potential to improve environmental safety in herbicide applications. Oliveira et al.[11] and Carvalho et al. [75] observed herbicidal effects at 10- and 80-times lower doses for atrazine-loaded in PCL and zein nanoformulations, respectively, against mustard plants (*Brassica oleracea*). Takeshita et al. [15] observed similar results for MTZ, with 10-fold lower doses being

effective in the control of *Ipomoea grandifolia*. In addition to dose reduction, nanoscale biopolymer carriers can offer additional benefits. For example, Bombo et al. [76] described the transpiration pathways (stomata and hydathodes) as an alternative uptake pathway, compared to leaf diffusion pathway, for atrazine in plants with PCL nanoparticles. Importantly, in the current study, PCL showed more efficient delivery and weed control at lower doses than does PCL-lignin. However, lignin is a natural polymer that is more suitable for a safe-by-design herbicide formulation and did exert sufficient weed control until 21 DAA. Selective activity against the weed species also appears to be an important benefit for nanoformulation applications.

3.4.2 Metribuzin uptake and distribution from nanoformulations

Fluorescence analyses were only able to be carried out in *A. retroflexus* until 5 DAA due significant leaf damage beyond 7 DAA hampering slide preparation and microscopic evaluation. Qualitative FI images are presented in Figure S3, comparing fluorescence channels (rows) and treatments (columns). *A. retroflexus* showed high background fluorescence; however, differences in nanoparticle uptake were evident at all time points by FI quantification (Fig. 6a and 6b). Clear nanoparticle signals were observed in the leaves, particularly for PCL-lig-MTZ, with distribution in various plant structures. Specifically, most of the nanoparticles were detected in leaves. PCL-MTZ presented 89.23 FI more than water treatments and PCL-lig-MTZ 826.24 FI, after first 24 h from nanoparticles application. After 5 days, this difference that was 737.01 FI at 24 h. After 5 days, the nanoparticles uptake difference was 9.25 times higher for PCL-lig-MTZ than PLC- MTZ in 24 h; this difference became 4.54 times after 5 days, evidencing the greater entry of nanoparticles in the presence of lignin in the composition of nanoformulation. In the roots, the FI values were similar between nanoformulations, due to the exportation of nanoparticles from the root to the shoot. Nevertheless, PCL-MTZ showed effective weed control, although a different mechanism of distribution and release of MTZ within plants treated with nanoformulations seems likely.

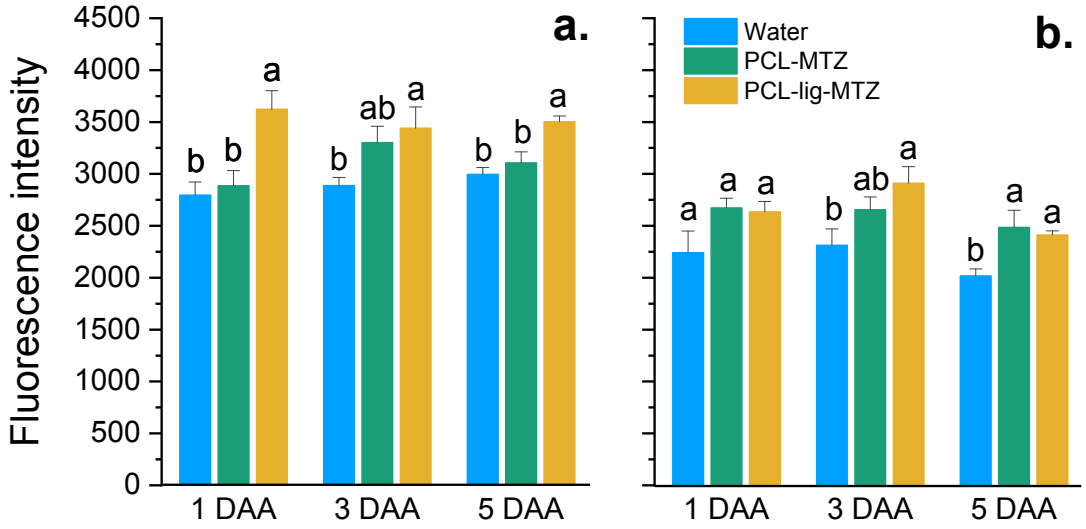

Figure 6. Fluorescence intensity (FI) of *Amaranthus retroflexus* plants at 5 days after application of metribuzin nanoencapsulated in two formulations (PCL-MTZ and PCL-lig-MTZ at 480 g a.i. ha^{-1}). Bars represent the mean and standard error mean of FI in the shoots (**a**) and roots (**b**). Different lowercase letters indicate statistically significant differences by Tukey's test ($p<0.05$; $n=5$) in the weed plant aerial part and roots.

The levels of metribuzin were below the limit of detection (<LOD); therefore, the total absorbed agrochemical was considered equal to the amount present in the shoots of the plants for quantification purposes. Non-significant interaction between "formulation" and "days after application" factors was observed by ANOVA (p<0,05). However, the formulations were different by Tukey's test (p<0,05; $n=12$, that represent all data over evaluation days). Less than 5% of the herbicide was absorbed by weed plants over 7 days. The herbicide uptake was 1.43 times higher after PCL-MTZ than after conventional MTZ in plants and 1.58 times higher than PCL-lig-MTZ, over 7 days. For PCL-lig-MTZ, the difference was only 0.91 times higher than conventional MTZ. Despite low uptake rate, metribuzin was efficiently to control *A. retroflexus*, independently of formulation. For nanoformulations, even at low dose (10-fold less than conventional; equivalent to 48 g a.i. ha^{-1}). Importantly, PCL-lig-MTZ exerted significant weed control, in spite of lower uptake rates. Given the greater sustainability of these nanoparticles, they can be considered a potentially more desirable nanocarrier of metribuzin than PCL-MTZ.

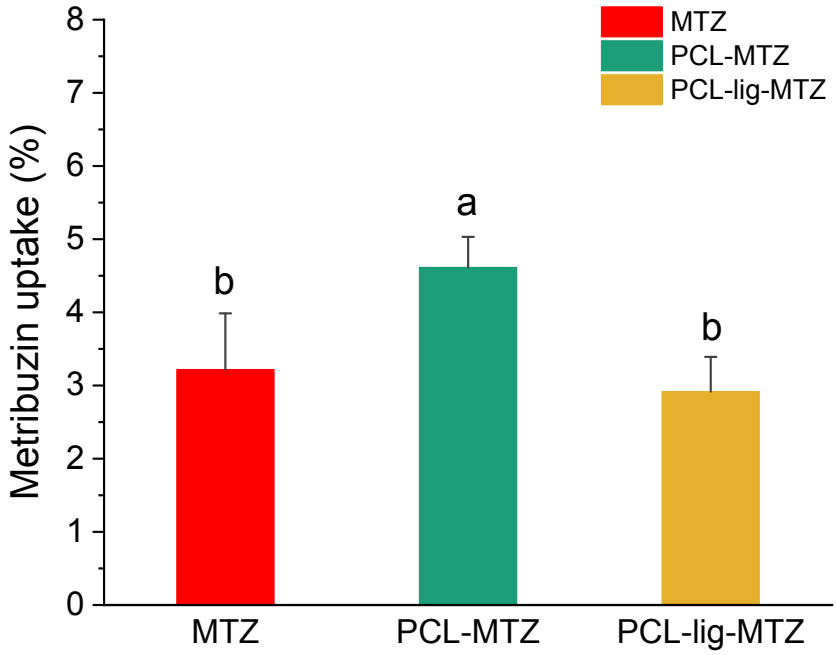

Figure 7. Metribuzin uptake in *Amaranthus retroflexus* plants over 7 days after application (DAA) of metribuzin non-encapsulated (MTZ) and nanoencapsulated in two formulations (PCL-MTZ and PCL-lig-MTZ at 480 g a.i. ha^{-1}). Bars represent the mean and standard error mean of treatments over 7 days after application. Different lowercase letters represent statistical differences by Tukey's test between treatments over evaluation days ($p<0.05$; $n=12$).

3.4.3 Photosynthetic and physiological damages

All photosynthetic parameters indicate damage from metribuzin in all formulations against *A. retroflexus* (Fig. 8). There was photosynthetic energy loss (PhiNO, PhiNPQ, and Phi2) and reduction in electron flow (LEF) caused by metribuzin, which is directly related to the known mechanism of action in plants (inhibitor of PSII), which is different from the soybean data. At 7 DAA, greater damage was observed for MTZ and PCL-MTZ as reflected in a reduced relative chlorophyll and linear electron flow. Nonetheless, the PCL-lig-MTZ showed photosynthetic damage comparable to all formulations on most evaluation days. As noted previously, the presence of lignin in nanoformulations increases the sustainability, biocompatibility, and safer for the environment as compared to synthetic carriers, even biodegradable ones such as PCL.

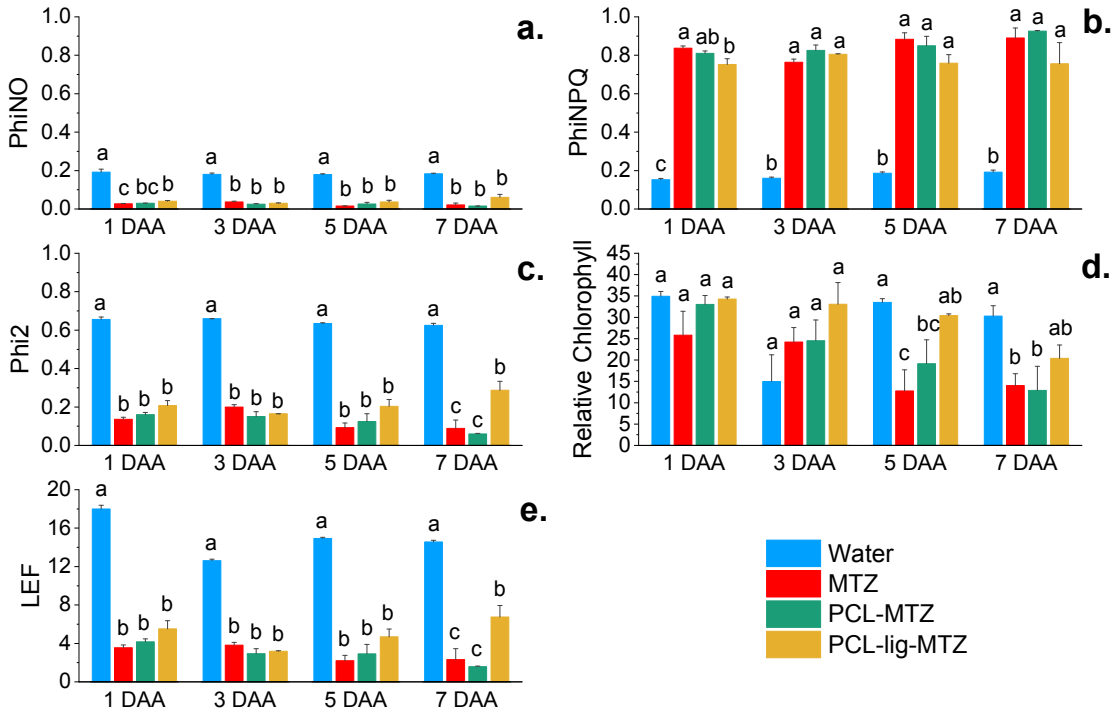

Figure 8. Photosynthetic parameters of *Amaranthus retroflexus* plants at 1, 3, 5, and 7 days after application of metribuzin non-encapsulated (MTZ) and nanoencapsulated in two formulations (PCL-MTZ and PCL-lig-MTZ at 480 g a.i. ha^{-1}). Bars represent the mean and standard error mean. Different lowercase letters represent statistical differences by Tukey's test between treatments on each evaluation day, on each parameter (p<0.05; n=6).

The detection of polymeric nanoparticles inside plants using fluorescence techniques has been described by some authors [40,76,77]. Here, despite a high background plant fluorescence signal (rhodamine B channel), it was possible to observe an accumulation of nanoparticles in the leaves, after translocation from the roots. We observed a strong correlation between nanoparticles and herbicide localization inside plant according to mass spectrometric analyses. Importantly, the current study was carried out in soil, simulating a natural environment for weed control. It is evident that even after soil interactions, the nanoscale formulations effectively delivered MTZ into the target plants. Additionally, the photosynthetic effects confirm that the delivery of MTZ was effective in the weed species, but led to minimal effects on the non-target species (soybean).

4. Conclusion

The findings of this study demonstrate that two nanoscale formulations of MTZ (178-265 nm) had effective weed control efficacy without significant impacts on non-

target soybean plants. Although there was a slight reduction on soybean shoot mass, a number of other physiological and biochemical indicators suggested minimal phytotoxicity. Importantly, PCL-MTZ and PCL-lig-MTZ were efficient in controlling *A. retroflexus* even at reduced dose (240 and 48 g a.i. ha^{-1}), compared to conventional MTZ (480 g a.i. ha^{-1}). The nanocarriers were absorbed by the plant roots and subsequently translocated to the shoot system, up to 1.43 higher than conventional MTZ. In addition, the nanoformulations has significant less impact on the soil microbiome, mitigating the alterations in the bacterial community caused by conventional MTZ (suppression effect). The ability of nanoformulations to precisely deliver MTZ to the target species could result in active ingredient reduction and decreased negative environmental impacts. Future work will evaluate this scenario under field conditions. Although PCL-lignin did not perform quite as well as PCL, from a safe-by-design approach, it may be more desirable. In fact, future work should focus on the use of lignin as a more sustainable alternative to other polymers for agricultural applications. Also, in further works, the effects of nanoparticles themselves may be explored to complement the information about the selectivity of nanoherbicides.

5. Acknowledgements

We would like to thank the Plant Pathology Department from the Connecticut Agricultural Experiment Station, for their kind support with the greenhouse, as well as Dr. Washington Da Silva' Lab. Additionally, we are grateful for funding from the Fundação de Amparo à Pesquisa de São Paulo (FAPESP, #2022/00509-0, #2019/04758-1, #2022/12221-0, #2022/12200-3, #2021/03455-5, #2022/01554-9, #2017/21004-5; CBioClima #2021/10639-5; #2022/16554-4), Brazilian National Council for Scientific and Technological Development (CNPq-MCTI-INCT NanoAgro #405924/2022-4, #308439/2021-0 L.F.F) and Coordenação de Aperfeiçoamento de Pessoal de Nível Superior – Brasil (CAPES-MEC INCTNanoAgro #88887.953443/2024-00), USDA National Institute of Food and Agriculture (#2022-08636), the National Science Foundation NSF EPSCoR Track 2 RII (OIA 1632854), and the USDA-NIFA Hatch (Project #1025564).

6. Authors contribution

V.T., and F.F.O.: investigation, methodology, writing - original draft; G.G., C.M.S., and C.A.: methodology; B.C.C, C.W.P, C.T., S.B, and J.L.: investigation, methodology; V.T.,

V.L.T., L.F.F., N.Z.M, C.D., and J.W.: conceptualization, writing - review & editing, supervision. All authors revised and have gave approval for the final version of the manuscript.

References

1 FAO, Pesticides use and trade 1990–2021, , DOI:10.4060/CC6958EN.

2 P. R. Ehrlich and J. Harte, Food security requires a new revolution, *International Journal of Environmental Studies*, 2015, **72**, 908–920.

3 R. Ofosu, E. D. Agyemang, A. Márton, G. Pásztor, J. Taller and G. Kazinczi, Herbicide Resistance: Managing Weeds in a Changing World, *Agronomy 2023, Vol. 13, Page 1595*, 2023, **13**, 1595.

4 F. Salinas, C. E. Astete, J. H. Waldvogel, S. Navarro, J. C. White, W. Elmer, C. Tamez, J. A. Davis and C. M. Sabliov, Effects of engineered lignin-graft-PLGA and zein-based nanoparticles on soybean health, *NanoImpact*, 2021, **23**, 100329.

5 X. Zhang, Y. He, Z. Yuan, G. Shen, Z. Zhang, J. Niu, L. He, J. Wang and K. Qian, A pH- and enzymatic-responsive nanopesticide to control pea aphids and reduce toxicity for earthworms, *Science of The Total Environment*, 2023, **861**, 160610.

6 J. Huang, J. Li, H. Chen, C. Shen and Y. Wen, Phytotoxicity alleviation of imazethapyr to non-target plant wheat: active regulation between auxin and DIMBOA, *Environ Sci Pollut Res Int*, 2023, **30**, 116004–116017.

7 M. Mehdizadeh, W. Mushtaq, S. A. Siddiqui, S. Ayadi, P. Kaur, S. Yeboah, S. Mazraedoost, D. K. A. Al-Taey and K. Tampubolon, Herbicide Residues in Agroecosystems: Fate, Detection, and Effect on Non-Target Plants, *Reviews in Agricultural Science*, 2021, **9**, 157–167.

8 R. Schulz, S. Bub, L. L. Petschick, S. Stehle and J. Wolfram, Applied pesticide toxicity shifts toward plants and invertebrates, even in GM crops, *Science (1979)*, 2021, **372**, 81–84.

9 L. F. Fraceto, R. Grillo, G. A. de Medeiros, V. Scognamiglio, G. Rea and C. Bartolucci, Nanotechnology in agriculture: Which innovation potential does it have?, *Front Environ Sci*, 2016, **4**, 186737.

10 M. Kah, A. K. Weniger and T. Hofmann, Impacts of (Nano)formulations on the Fate of an Insecticide in Soil and Consequences for Environmental Exposure Assessment, *Environ Sci Technol*, 2016, **50**, 10960–10967.

11 H. C. Oliveira, R. Stolf-Moreira, C. B. R. Martinez, R. Grillo, M. B. De Jesus and L. F. Fraceto, Nanoencapsulation Enhances the Post-Emergence Herbicidal Activity of Atrazine against Mustard Plants, *PLoS One*, 2015, **10**, e0132971.

12 M. Pascoli, P. J. Lopes-Oliveira, L. F. Fraceto, A. B. Seabra and H. C. Oliveira, State of the art of polymeric nanoparticles as carrier systems with agricultural applications: a minireview, *Energy Ecol Environ*, 2018, **3**, 137–148.

13 A. D. E. S. Pereira, H. C. Oliveira, L. F. Fraceto and C. Santaella, Nanotechnology potential in seed priming for sustainable agriculture, *Nanomaterials*, 2021, **11**, 1–29.

14 J. Dong, X. Liu, Y. Chen, W. Yang and X. Du, User-safe and efficient chitosan-gated porous carbon nanopesticides and nanoherbicides, *J Colloid Interface Sci*, 2021, **594**, 20–34.

15 V. Takeshita, L. B. Carvalho, J. A. Galhardi, G. V. Munhoz-Garcia, R. F. Pimpinato, H. C. Oliveira, V. L. Tornisielo and L. F. Fraceto, Development of a Preemergent Nanoherbicide: From Efficiency Evaluation to the Assessment of Environmental Fate and Risks to Soil Microorganisms, *ACS Nanoscience Au*, 2022, **2**, 307–323.

16 R. Hou, J. Zhou, Z. Song, N. Zhang, S. Huang, A. E. Kaziem, C. Zhao and Z. Zhang, pH-responsive λ-cyhalothrin nanopesticides for effective pest control and reduced toxicity to Harmonia axyridis, *Carbohydr Polym*, 2023, **302**, 120373.

17 M. Zargar, M. Bayat, F. S. Saquee, S. Diakite, N. M. Ramzanovich and K. A. S. Akhmadovich, New Advances in Nano-Enabled Weed Management Using Poly(Epsilon-Caprolactone)-Based Nanoherbicides: A Review, *Agriculture 2023, Vol. 13, Page 2031*, 2023, **13**, 2031.

18 R. Grillo, N. Z. P. dos Santos, C. R. Maruyama, A. H. Rosa, R. de Lima and L. F. Fraceto, Poly(e{open}-caprolactone)nanocapsules as carrier systems for herbicides: Physico-chemical characterization and genotoxicity evaluation, *J Hazard Mater*, 2012, **231–232**, 1–9.

19 C. R. Maruyama, M. Guilger, M. Pascoli, N. Bileshy-José, P. C. Abhilash, L. F. Fraceto and R. De Lima, Nanoparticles Based on Chitosan as Carriers for the Combined Herbicides Imazapic and Imazapyr, *Sci Rep*, , DOI:10.1038/srep19768.

20 J. Oliveira, E. V. R. Campos, A. E. S. Pereira, T. Pasquoto, R. Lima, R. Grillo, D. J. De Andrade, F. A. Dos Santos and L. F. Fraceto, Zein Nanoparticles as Eco-

Friendly Carrier Systems for Botanical Repellents Aiming Sustainable Agriculture, *J Agric Food Chem*, 2018, **66**, 1330–1340.

21 R. Grillo, L. F. Fraceto, M. J. B. Amorim, J. J. Scott-Fordsmand, R. Schoonjans and Q. Chaudhry, Ecotoxicological and regulatory aspects of environmental sustainability of nanopesticides, *J Hazard Mater*, , DOI:10.1016/j.jhazmat.2020.124148.

22 P. Mandal and R. Shunmugam, Polycaprolactone: a biodegradable polymer with its application in the field of self-assembly study, *Journal of Macromolecular Science, Part A: Pure and Applied Chemistry*, 2020, **58**, 111–129.

23 V. Takeshita, G. V. Munhoz-Garcia, C. Werk Pinácio, B. C. Cardoso, D. Nalin, V. L. Tornisielo and L. F. Fraceto, Availability of Metribuzin-Loaded Polymeric Nanoparticles in Different Soil Systems: An Important Study on the Development of Safe Nanoherbicides, *Plants*, 2022, **11**, 3366.

24 V. Takeshita, B. T. de Sousa, A. C. Preisler, L. B. Carvalho, A. do E. S. Pereira, V. L. Tornisielo, G. Dalazen, H. C. Oliveira and L. F. Fraceto, Foliar absorption and field herbicidal studies of atrazine-loaded polymeric nanoparticles, *J Hazard Mater*, 2021, **418**, 126350.

25 M. Li, Y. Pu, F. Chen and A. J. Ragauskas, Synthesis and Characterization of Lignin-grafted-poly(ε-caprolactone) from Different Biomass Sources, *N Biotechnol*, 2021, **60**, 189–199.

26 A. Garcia, C. E. Astete, R. Cueto and C. M. Sabliov, Modulation of Methoxyfenozide Release from Lignin Nanoparticles Made of Lignin Grafted with PCL by ROP and Acylation Grafting Methods, *Langmuir*, 2024, **40**, 5433–5443.

27 C. Tamez, M. Molina-Hernandez, I. A. Medina-Velo, K. Cota-Ruiz, J. A. Hernandez-Viezcas and J. Gardea-Torresdey, Long-term assessment of nano and bulk copper compound exposure in sugarcane (Saccharum officinarum), *Science of The Total Environment*, 2020, **718**, 137318.

28 C. Ma, H. Liu, G. Chen, Q. Zhao, B. Eitzer, Z. Wang, W. Cai, L. A. Newman, J. C. White, O. P. Dhankher and B. Xing, Effects of titanium oxide nanoparticles on tetracycline accumulation and toxicity in Oryza sativa (L.), *Environ Sci Nano*, 2017, **4**, 1827–1839.

29 C. Ma, S. Chhikara, B. Xing, C. Musante, J. C. White and O. P. Dhankher, Physiological and molecular response of arabidopsis thaliana (L.) to nanoparticle cerium and indium oxide exposure, *ACS Sustain Chem Eng*, 2013, **1**, 768–778.

30 I. A. Medina-Velo, N. Zuverza-Mena, C. Tamez, Y. Ye, J. A. Hernandez-Viezcas, J. C. White, J. R. Peralta-Videa and J. L. Gardea-Torresdey, Minimal Transgenerational Effect of ZnO Nanomaterials on the Physiology and Nutrient Profile of Phaseolus vulgaris, *ACS Sustain Chem Eng*, 2018, **6**, 7924–7930.

31 C. Ma, S. Chhikara, B. Xing, C. Musante, J. C. White and O. P. Dhankher, Physiological and molecular response of arabidopsis thaliana (L.) to nanoparticle cerium and indium oxide exposure, *ACS Sustain Chem Eng*, 2013, **1**, 768–778.

32 D. K. Hazra, A. Purkait, D. Raghuwanshi and K. Sri Rama Murthy, Method Validation for Quantitative Analysis of Metribuzin in Wheat by Liquid Chromatography–Tandem Mass Spectrometry, *J Chromatogr Sci*, 2021, **59**, 47–54.

33 W. M. A. Sillen, S. Thijs, G. R. Abbamondi, R. De La Torre Roche, N. Weyens, J. C. White and J. Vangronsveld, Nanoparticle treatment of maize analyzed through the metatranscriptome: Compromised nitrogen cycling, possible phytopathogen selection, and plant hormesis, *Microbiome*, 2020, **8**, 1–17.

34 E. S. Wright and K. H. Vetsigian, Quality filtering of Illumina index reads mitigates sample cross-talk, *BMC Genomics*, 2016, **17**, 1–7.

35 M. Sakai and M. Ikenaga, Application of peptide nucleic acid (PNA)-PCR clamping technique to investigate the community structures of rhizobacteria associated with plant roots, *J Microbiol Methods*, 2013, **92**, 281–288.

36 S. J. Taerum, B. Steven, D. J. Gage and L. R. Triplett, Validation of a PNA clamping method for reducing host DNA amplification and increasing eukaryotic diversity in rhizosphere microbiome studies, *Phytobiomes J*, 2020, **4**, 291–302.

37 P. D. Schloss, S. L. Westcott, T. Ryabin, J. R. Hall, M. Hartmann, E. B. Hollister, R. A. Lesniewski, B. B. Oakley, D. H. Parks, C. J. Robinson, J. W. Sahl, B. Stres, G. G. Thallinger, D. J. Van Horn and C. F. Weber, Introducing mothur: Open-source, platform-independent, community-supported software for describing and comparing microbial communities, *Appl Environ Microbiol*, 2009, **75**, 7537–7541.

38 C. Quast, E. Pruesse, P. Yilmaz, J. Gerken, T. Schweer, P. Yarza, J. Peplies and F. O. Glöckner, The SILVA ribosomal RNA gene database project: improved data processing and web-based tools, *Nucleic Acids Res*, 2013, **41**, D590.

39 Q. Wang, G. M. Garrity, J. M. Tiedje and J. R. Cole, Naïve Bayesian classifier for rapid assignment of rRNA sequences into the new bacterial taxonomy, *Appl Environ Microbiol*, 2007, **73**, 5261–5267.

40 A. C. Preisler, L. B. Carvalho, T. Saraiva-Santos, W. A. Verri, J. L. S. Mayer, L. F. Fraceto, G. Dalazen and H. C. Oliveira, Interaction of Nanoatrazine and Target Organism: Evaluation of Fate and Photosystem II Inhibition in Hydroponically Grown Mustard (Brassica juncea) Plants, *J Agric Food Chem*, 2022, **70**, 7644–7652.

41 P. J. McMurdie and S. Holmes, phyloseq: An R Package for Reproducible Interactive Analysis and Graphics of Microbiome Census Data, *PLoS One*, 2013, **8**, e61217.

42 P. Dixon, VEGAN, a package of R functions for community ecology, *Journal of Vegetation Science*, 2003, **14**, 927–930.

43 Y. Cao, Q. Dong, D. Wang, P. Zhang, Y. Liu and C. Niu, microbiomeMarker: an R/Bioconductor package for microbiome marker identification and visualization, *Bioinformatics*, 2022, **38**, 4027–4029.

44 N. Segata, J. Izard, L. Waldron, D. Gevers, L. Miropolsky, W. S. Garrett and C. Huttenhower, Metagenomic biomarker discovery and explanation, *Genome Biol*, 2011, **12**, 1–18.

45 R. Grillo, A. E. S. Pereira, C. S. Nishisaka, R. De Lima, K. Oehlke, R. Greiner and L. F. Fraceto, Chitosan/tripolyphosphate nanoparticles loaded with paraquat herbicide: An environmentally safer alternative for weed control, *J Hazard Mater*, 2014, **278**, 163–171.

46 D. M. Kramer, G. Johnson, O. Kiirats and G. E. Edwards, New fluorescence parameters for the determination of QA redox state and excitation energy fluxes, *Photosynth Res*, 2004, **79**, 209–218.

47 S. Kuhlgert, G. Austic, R. Zegarac, I. Osei-Bonsu, D. Hoh, M. I. Chilvers, M. G. Roth, K. Bi, D. TerAvest, P. Weebadde and D. M. Kramer, MultispeQ Beta: a tool for large-scale plant phenotyping connected to the open PhotosynQ network, *R Soc Open Sci*, , DOI:10.1098/RSOS.160592.

48 M. Moustakas, J. Moustaka and I. Sperdouli, Hormesis in photosystem II: a mechanistic understanding, *Curr Opin Toxicol*, 2022, **29**, 57–64.

49 M. A. Gabr, M. A. Shakeeb and I. M. Zid, Metabolic changes associated with growth of soybean as affected by pre-emergence application of metribuzin. Canadian Journal of Botany, 66(12), 2380–2384 | 10.1139/b88-323, *Canadian Journal of Botany, 66(12)*, 1988, 2380–2384.

50 B. L. Mageot, F. Slife and C. E. Rieck, Differential Metabolism of Metribuzin by Two Soybean (Glycine max) Cultivars. Weed Science, 27(3), 267–269 | 10.1017/s0043174500043988, https://doi.org/10.1017/s0043174500043988, (accessed 5 June 2023).

51 C. Fedtke and R. R. Schmidt, BEHAVIOUR OF METRIBUZIN IN TOLERANT AND SUSCEPTIBLE SOYBEAN VARIETIES, *Mode of Action, Metabolism and Toxicology*, 1983, 177–182.

52 D. S. Frear, H. R. Swanson and E. R. Mansager, Alternate pathways of metribuzin metabolism in soybean: Formation of N-glucoside and homoglutathione conjugates, *Pestic Biochem Physiol*, 1985, **23**, 56–65.

53 Irsad, N. Talreja, D. Chauhan, R. V. Mangalaraja, P. Q. Rizvi and M. Ashfaq, Polymeric Composites: A Promising Tool for Enhancing Photosyntheticy Efficiency of Crops, *Metabolic Engineering in Plants*, 2022, 341–357.

54 V. Demidchik, Mechanisms of oxidative stress in plants: From classical chemistry to cell biology, *Environ Exp Bot*, 2015, **109**, 212–228.

55 D. Y. Nakasato, A. E. S. Pereira, J. L. Oliveira, H. C. Oliveira and L. F. Fraceto, Evaluation of the effects of polymeric chitosan/tripolyphosphate and solid lipid nanoparticles on germination of Zea mays, Brassica rapa and Pisum sativum, *Ecotoxicol Environ Saf*, 2017, **142**, 369–374.

56 T. Kacsó, E. A. Hanna, F. Salinas, C. E. Astete, E. Bodoki, R. Oprean, P. P. Price, V. P. Doyle, C. A. R. Bonser, J. A. Davis and C. M. Sabliov, Zein and lignin-based nanoparticles as soybean seed treatment: translocation and impact on seed and plant health, *Applied Nanoscience (Switzerland)*, 2022, **12**, 1557–1569.

57 H. C. Oliveira, R. Stolf-Moreira, C. B. R. Martinez, G. F. M. Sousa, R. Grillo, M. B. de Jesus and L. F. Fraceto, Evaluation of the side effects of poly(epsilon-caprolactone) nanocapsules containing atrazine toward maize plants, *Front Chem*, 2015, **3**, 164987.

58 M. Morales and S. Munné-Bosch, Malondialdehyde: Facts and Artifacts, *Plant Physiol*, 2019, **180**, 1246–1250.

59 A. C. Preisler, A. E. S. Pereira, E. V. R. Campos, G. Dalazen, L. F. Fraceto and H. C. Oliveira, Atrazine nanoencapsulation improves pre-emergence herbicidal activity against Bidens pilosa without enhancing long-term residual effect on Glycine max, *Pest Manag Sci*, 2020, **76**, 141–149.

60 A. E. S. Pereira, R. Grillo, N. F. S. Mello, A. H. Rosa and L. F. Fraceto, Application of poly(epsilon-caprolactone) nanoparticles containing atrazine herbicide as an alternative technique to control weeds and reduce damage to the environment, *J Hazard Mater*, 2014, **268**, 207–215.

61 S. Kumar, D. Kumar and N. Dilbaghi, Preparation, characterization, and bio-efficacy evaluation of controlled release carbendazim-loaded polymeric nanoparticles, *Environmental Science and Pollution Research*, 2017, **24**, 926–937.

62 Y. Tong, Y. Wu, C. Zhao, Y. Xu, J. Lu, S. Xiang, F. Zong and X. Wu, Polymeric Nanoparticles as a Metolachlor Carrier: Water-Based Formulation for Hydrophobic Pesticides and Absorption by Plants, *J Agric Food Chem*, 2017, **65**, 7371–7378.

63 G. D. Bending, S. D. Lincoln, S. R. Sørensen, J. A. W. Morgan, J. Aamand and A. Walker, In-Field Spatial Variability in the Degradation of the Phenyl-Urea Herbicide Isoproturon Is the Result of Interactions between Degradative Sphingomonas spp. and Soil pH, *Appl Environ Microbiol*, 2003, **69**, 827.

64 A. Heydari and I. J. Misaghi, Biocontrol activity of Burkholderia cepacia against Rhizoctonia solani in herbicide-treated soils on JSTOR, https://www.jstor.org/stable/42948348, (accessed 4 June 2023).

65 C. S. Jacobsen, Plant protection and rhizosphere colonization of barley by seed inoculated herbicide degrading Burkholderia (Pseudomonas) cepacia DBO1(pRO101) in 2,4-D contaminated soil, *Plant Soil*, 1997, **189**, 139–144.

66 Z. Lü, H. Min, S. Wu and A. Ruan, Phylogenetic and degradation characterization of Burkholderia cepacia WZ1 degrading herbicide quinclorac, *J Environ Sci Health B*, 2003, **38**, 771–782.

67 S. R. Sørensen, Z. Ronen and J. Aamand, Isolation from Agricultural Soil and Characterization of a Sphingomonas sp. Able To Mineralize the Phenylurea Herbicide Isoproturon, *Appl Environ Microbiol*, 2001, **67**, 5403.

68 J. A. Galhardi, L. F. Fraceto, K. J. Wilkinson and S. Ghoshal, Soil Enzyme Activities as an Integral Part of the Environmental Risk Assessment of Nanopesticides, *J Agric Food Chem*, 2020, **68**, 8514–8516.

69 Y. Zhai, F. Abdolahpur Monikh, J. Wu, R. Grillo, D. Arenas-Lago, G. K. Darbha, M. G. Vijver and W. J. G. M. Peijnenburg, Interaction between a nano-formulation of atrazine and rhizosphere bacterial communities: atrazine degradation and bacterial community alterations, *Environ Sci Nano*, 2020, **7**, 3372–3384.

70 W. Liu, J. Yao, M. Cai, H. Chai, C. Zhang, J. Sun, R. Chandankere and K. Masakorala, Synthesis of a novel nanopesticide and its potential toxic effect on soil microbial activity, *Journal of Nanoparticle Research*, 2014, **16**, 1–13.

71 V. Bueno, P. Wang, O. Harrisson, S. Bayen and S. Ghoshal, Impacts of Porous Silica-Nanoencapsulated Pesticide Applied to Soil on Plant Growth and Soil Microbial Community, , DOI:10.26434/CHEMRXIV-2021-RT454.

72 S. Prudnikova, N. Streltsova and T. Volova, The effect of the pesticide delivery method on the microbial community of field soil, *Environmental Science and Pollution Research 2020 28:7*, 2020, **28**, 8681–8697.

73 P. Shan, Y. Lu, W. Lu, X. Yin, H. Liu, D. Li, X. Lian, W. Wang, Z. Li and Z. Li, Biodegradable and Light-Responsive Polymeric Nanoparticles for Environmentally Safe Herbicide Delivery, *ACS Appl Mater Interfaces*, 2022, **14**, 43759–43770.

74 S. I. L. Gomes, J. J. Scott-Fordsmand, E. V. R. Campos, R. Grillo, L. F. Fraceto and M. J. B. Amorim, On the safety of nanoformulations to non-target soil invertebrates – an atrazine case study, *Environ Sci Nano*, 2019, **6**, 1950–1958.

75 L. B. Carvalho, I. S. Godoy, A. C. Preisler, P. L. de Freitas Proença, T. Saraiva-Santos, W. A. Verri, H. C. Oliveira, G. Dalazen and L. F. Fraceto, Pre-emergence herbicidal efficiency and uptake of atrazine-loaded zein nanoparticles: a sustainable alternative to weed control, *Environ Sci Nano*, 2023, **10**, 1629–1643.

76 A. B. Bombo, A. E. S. Pereira, M. G. Lusa, E. De Medeiros Oliveira, J. L. De Oliveira, E. V. R. Campos, M. B. De Jesus, H. C. Oliveira, L. F. Fraceto and J. L. S. Mayer, A Mechanistic View of Interactions of a Nanoherbicide with Target Organism, *J Agric Food Chem*, 2019, **67**, 4453–4462.

77 K. D. Ristroph, C. E. Astete, E. Bodoki and C. M. Sabliov, Zein Nanoparticles Uptake by Hydroponically Grown Soybean Plants, *Environ Sci Technol*, 2017, **51**, 14065–14071.

Delivering metribuzin from biodegradable nanocarriers: Assessing herbicidal effects for soybean plant protection and weed control

Vanessa Takeshita[1*]; Felipe F. Oliveira[2]; Alvaro Garcia[3]; Nubia Zuverza-Mena[4]; Carlos Tamez[4]; Brian C. Cardoso[1]; Camila W. Pinácio[1]; Blaire Steven[5]; Jacquelyn LaReau[5]; Carlos E. Astete[3]; Cristina M. Sabliov[3]; Leonardo F. Fraceto[6]; Valdemar L. Tornisielo[1]; Christian O. Dimkpa[4]; Jason C. White[4]

[1]Center of Nuclear Energy in Agriculture, University of São Paulo, Piracicaba, SP 13416-000, Brazil; [2]Department of Plant Pathology & Nematology, Superior School of Agriculture "Luiz de Queiroz", University of São Paulo, Piracicaba, SP 13418-900, Brazil; [3]Biological & Agricultural Engineering, Louisiana State University and LSU Ag Center, Baton Rouge, LA 70808, United States; [4]Department of Analytical Chemistry, The Connecticut Agricultural Experiment Station, New Haven, CT 06511, United States; [5]Department Environmental Science and Forestry, The Connecticut Agricultural Experiment Station, New Haven, CT 06504, United States; [6]Institute of Science and Technology, São Paulo State University (UNESP), Sorocaba, SP 18087-180, Brazil.

*Correspondent author: vanessatakeshita@usp.br and vanessatakeshita@gmail.com

Data availability

Data for this article are available at [Zenodo] at [https://doi.org/10.5281/zenodo.13386458].